

Some Results of Modeling the Propagation of a Hydrogen Flame in a Narrow Annular Gap of a Piston Engine Combustion Chamber

Revaz Kavtaradze*

*Rafael Dvali Institute of Machine Mechanics (IMM)
10 Mindeli St., Tbilisi, 0186, Georgia*

Some results of mathematical modeling of the process of hydrogen flame propagation in the gap between the piston and the cylinder of a hydrogen engine are presented. A mathematical model of intra-cylinder turbulent processes based on fundamental Navier-Stokes type equations is presented, which are solved using the numerical control volume method. As a result, the phenomenon of increased heat loss in hydrogen engines is explained, which was previously observed in experimental studies by a number of authors who did not provide a theoretical analysis of this phenomenon. It is shown that one of the main reasons for the increase in heat losses is the propagation of a hydrogen flame in a narrow annular gap between the piston and the cylinder located above the compression ring of the piston. The heat exchange process in the gap is modeled and thermal boundary conditions (coefficients of unsteady heat transfer) on the surfaces of the piston and cylinder are determined. Temperature and velocity fields, as well as hydrogen concentrations, characterizing the dynamics of flame development are obtained. It has been found that in cases of penetration and extinguishing of a hydrogen flame, the heat losses in the combustion chamber and the thermal loads on the main parts, primarily on the piston and cylinder liner, differ significantly from each other. The possibility of controlling the process of flame propagation into the gap and reducing heat losses by regulating the size of the gap and the composition of the hydrogen-air mixture is indicated. This should be taken into account in practice, especially when converting serial engines running on traditional hydrocarbon fuels to hydrogen.

Keywords and phrases: Modeling, turbulence, hydrogen engine, flame propagation, annular gap, heat transfer.

AMS subject classification: 80A05, 35Q30.

1 Introduction. The state of the problem

The conversion of modern piston engines, the main consumers of hydrocarbon fuels, to hydrogen contributes to solving such global problems of modern civilization as energy, environmental and climate problems. High values of the heat of hydrogen combustion, flame propagation and heat release rates, as well as wide ignition concentration limits of the hydrogen-air mixture can lead to thermo-physical phenomena not typical for traditional engines running on hydrocarbon fuels (natural gas, gasoline, diesel fuel).

One of the features of the intra-cylinder processes of a hydrogen engine is associated with the processes of unsteady heat exchange in the combustion chamber. Experimental studies by T. Scudo [1, 2] and J. Demuyne et al. [3] have shown that the combustion of hydrogen leads to a more intensive transfer of heat to the walls of the combustion chamber, i.e. to higher heat

*Corresponding author. Email: rzkavtaradze@gmail.com

losses compared with the combustion of hydrocarbon fuels. At the same time, the value of the heat transfer coefficient during stoichiometric combustion of hydrogen is 4 times higher than during the combustion of gasoline, and 2 times higher than during the combustion of natural gas (CH_4). In this regard, in formulas known from the theory of reciprocating engines for calculating the heat transfer coefficient, for example, in the G. Woschni formula, appropriate correction coefficients are introduced [1].

The main reason for the phenomenon of increased heat losses in the combustion chamber of a hydrogen engine, these authors consider, first of all, the high rate of hydrogen combustion. Without denying the role of the hydrogen combustion rate in increasing the intensity of heat transfer to the walls of the combustion chamber, we note that it is necessary to establish the cause of this phenomenon and its clearer theoretical interpretation, supported by quantitative data. This article develops the hypothesis proposed by the author in [4], according to which the main reason for this phenomenon is the ability of a hydrogen flame to penetrate into micro gaps of this size, at the entrance of which the flame of a hydrocarbon fuel goes out.

The effect of the critical size ℓ_{cr} of hydrogen flame quenching on the process of heat exchange with the walls of the combustion chamber is investigated on the basis of classical results obtained by Ya. B. Zeldovich [5]. Note that ℓ_{cr} is a characteristic parameter of the combustible mixture at certain values of pressure and temperature [6]. When a flame spreads in a pipe (in a gap, in an annular channel, etc.), ℓ_{cr} is equal to the minimum inner diameter of the pipe (the size of the gap, the distance between the walls of the annular channel, etc.) at which the flame of a gaseous combustible mixture can still mix in the pipe without obstruction (in the gap, in the annular channel, etc.). Its values are: for a gasoline-air mixture, $\ell_{crH2} > 0,25mm$; for a hydrogen-air mixture, $\ell_{cr} = 0,06mm$, i.e. the penetration capacity of a hydrogen flame into the pipe is approximately 4,2 times greater than that of a gasoline flame [7, 8, 9].

It was found in [4] that in the conditions of the combustion chamber of reciprocating engines, the critical size of the hydrogen flame quenching is $\ell_{crH2} \approx 0.125mm$, and the flame of hydrocarbon fuels is $\ell_{crCH} \approx 0.5mm$. This article examines the annular gap between the piston and the cylinder, located above the compression ring and adjacent to the total volume of the combustion chamber. The gap has the following dimensions: width $\ell = 0.2mm$, and height $h = 5mm$ (Fig. 1). These dimensions were established by measuring on a hot experimental serial gasoline engine of Chinese production CA20, converted to hydrogen. Note that the experimental hydrogen engine has the following parameters: number of cylinders 4, cylinder diameter/piston stroke $D/S = 86/86mm/mm$, compression ratio $\varepsilon = 10$, power $Ne = 60kW$ (at rotation speed $n = 5500min^{-1}$), torque $Mmax = 111Nm$ (at $n = 4000min^{-1}$). Thus, the size of the annular gap ℓ in the combustion chamber in the hot state of the hydrogen engine under study satisfies the condition

$$\ell_{crCH} > \ell > \ell_{crH2}. \quad (1)$$

Condition (1) means that on a real engine, the hydrogen flame penetrates and spreads into the gap, and the flame of hydrocarbon fuel (CH_4 , gasoline, diesel fuel, etc.) cannot penetrate into the gap and goes out. In order to prove this statement, some results of mathematical modeling of the propagation of a hydrogen flame in the gap are given below and the conditions for its extinguishing are indicated. It should also be noted that direct measurements of such characteristic flame parameters as the front velocity and temperature, as well as visual observation of the processes of its propagation/extinguishing in a narrow annular gap in the cylinder of a running engine, is a difficult, as yet unfulfilled task.

2 A brief description of the mathematical model

Fig. 1 shows the axial cross-section of a three-dimensional cylinder design of a reciprocating engine. Let's introduce some definitions: The total firing surface of the piston is the area where heat transfer from the burning gas (from the flame) F_{TFP} occurs. This area is equal to the sum of the upper firing surface of the piston F_{UFP} and the lateral firing surface of the piston, i.e. the surface of the piston firing belt F_{SFP} , with $F_{TFP} = F_{UFP} + F_{SFP}$. The total internal firing surface of the annular gap F_{TFG} consists of the surfaces of the firing belt of the piston F_{SFP} , the firing belt of the cylinder liner F_{SFZ} and the upper surface of the piston ring F_{OFR} , i.e. $F_{TFG} = F_{SFP} + F_{SFZ} + F_{OFR}$.

Note that for the specific case under consideration ($l = 0.2mm, h = 5m$), the area of the total inner firing surface of the F_{TFG} annular gap is 32% of the area of the total firing surface of the piston. Since the flame of hydrocarbon fuels will not be able to penetrate into a gap with a size of $l = 0.2mm$, the inner surface of the gap with an area of F_{TFG} cannot be called a firing and, of course, it is not a surface of intensive heat exchange. Obviously, the presence or absence of intense heat exchange in the area F_{TFG} has a significant effect on heat losses, as well as on the thermal condition of the piston.

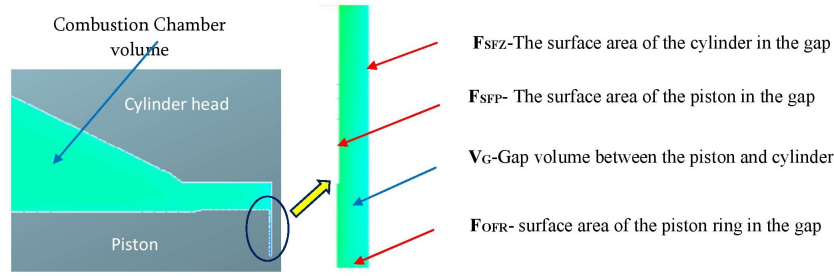


Figure 1: The combustion chamber and the annular gap between the piston and the cylinder above the upper piston ring (axial section). F_{SFZ} -The surface of the cylinder in the gap, F_{SFP} -The surface of the piston in the gap, F_{OFR} - surface of the piston ring in the gap, V_G -Gap volume between the piston and cylinder.

The thermal-physical processes (movement of the working fluid, ignition and combustion of the mixture, as well as heat generation, formation of nitrogen oxides and heat transfer with the walls) occurring in the combustion chamber and the adjacent gap are investigated using a three-dimensional mathematical model. The model is based on the fundamental equations of momentum (Navier-Stokes equations), energy (Fourier-Kirchhoff equation), diffusion (Fick equation) and continuity equation (see Table 1). In these equations, the current time τ is related to the angle φ of rotation of the engine crankshaft by the expression $\varphi = \omega\tau$, where $\omega = \pi n/30$ is the angular velocity and n is the rotational speed of the crankshaft. Since for an arbitrary high-speed mode of operation, $\omega = const$, the parameters φ and τ uniquely determine the angle of rotation of the crankshaft and the corresponding torque, i.e. in this sense, these terms are identical.

The following designations are used in the equations from Table 1: p - is pressure, N/m^2 ; G_i - the projection of the vector of the density of volumetric forces on the Ox_i axis of the rectangular Cartesian coordinate system, N/m^3 ; \vec{W} is the vector of gas velocity, m/s ; ρ is the density of gas,

Table 1

The main equations of a mathematical model of the working process of a hydrogen diesel engine		
EQUATIONS OF LAWS OF CONSERVATION AS PARTICULAR CASES OF THE GENERALIZED DIFFERENTIAL EQUATION		
$\frac{\partial}{\partial \tau}(\rho \Phi) + \text{div}(\rho \vec{W} \Phi) = \text{div}(\Gamma_{\Phi} \text{grad} \Phi) + S_{\Phi} \Leftrightarrow \frac{\partial}{\partial \tau}(\rho \Phi) + \frac{\partial}{\partial x_j}(\rho W_j \Phi) = \frac{\partial}{\partial x_j} \left(\Gamma_{\Phi} \frac{\partial \Phi}{\partial x_j} \right) + S_{\Phi}$		
$\Phi = W_i, \Gamma_{\Phi} = \mu,$ $S_{\Phi} = G_i - \frac{\partial p}{\partial x_i} + V_{\mu},$ Equation of conservation of the momentum (Navier-Stokes equation)	Initial form	$\rho \frac{DW_i}{D\tau} = G_i - \frac{\partial p}{\partial x_i} + \frac{\partial}{\partial x_j} \left[\mu \left(\frac{\partial W_i}{\partial x_j} + \frac{\partial W_j}{\partial x_i} - \frac{2}{3} \delta_{ij} \frac{\partial W_k}{\partial x_k} \right) \right]$
	Reynolds form	$\bar{\rho} \frac{D\bar{W}_i}{D\tau} = \bar{G}_i - \frac{\partial \bar{p}}{\partial x_i} + \frac{\partial}{\partial x_j} \left[\bar{\mu} \left(\frac{\partial \bar{W}_i}{\partial x_j} + \frac{\partial \bar{W}_j}{\partial x_i} - \frac{2}{3} \delta_{ij} \frac{\partial \bar{W}_k}{\partial x_k} \right) - \bar{\rho} \bar{W}'_i \bar{W}'_j \right]$
	New unknown quantities	$\bar{\rho} \bar{W}'_i \bar{W}'_j$ - tensor of the Reynolds turbulent stresses determined by the oscillatory components of velocity; $\bar{\tau}_{ij} = \bar{\mu} \left(\frac{\partial \bar{W}_i}{\partial x_j} + \frac{\partial \bar{W}_j}{\partial x_i} - \frac{2}{3} \delta_{ij} \frac{\partial \bar{W}_k}{\partial x_k} \right)$ - tensor of the viscous (turbulent) stresses determined by the averaged values of the velocity components.
$\Phi = H, \Gamma_{\Phi} = \frac{\lambda}{c_p},$ $S_{\Phi} = \frac{\partial p}{\partial \tau} + \frac{\partial}{\partial x_i}(\tau_{ij} W_j) + G_j W_j + w_r Q_r + \frac{\partial q_{Rj}}{\partial x_j}$ Energy conservation equation	Initial form	$\rho \frac{DH}{D\tau} = G_j W_j + \frac{\partial p}{\partial \tau} + \frac{\partial}{\partial x_i}(\tau_{ij} W_j) + \frac{\partial}{\partial x_j} \left(\lambda \frac{\partial T}{\partial x_j} \right) + w_r Q_r + \frac{\partial q_{Rj}}{\partial x_j}$
	Reynolds form	$\bar{\rho} \frac{D\bar{H}}{D\tau} = \bar{G}_j \bar{W}_j + \frac{\partial \bar{p}}{\partial \tau} + \frac{\partial}{\partial x_j}(\bar{\tau}_{ij} \bar{W}_j) + \frac{\partial}{\partial x_j} \left(\bar{\lambda} \frac{\partial \bar{T}}{\partial x_j} - c_p \bar{\rho} \bar{T}' \bar{W}'_j \right) + \bar{w}_r \bar{Q}_r + \frac{\partial \bar{q}_{Rj}}{\partial x_j}$
$\Phi = 1, \Gamma_{\Phi} = 0, S_{\Phi} = 0$ Mass (continuity) conservation equation	Initial form	$\frac{\partial \rho}{\partial \tau} + \frac{\partial}{\partial x_j}(\rho W_j) = 0$
	Reynolds form	$\frac{\partial \bar{\rho}}{\partial \tau} + \frac{\partial}{\partial x_j}(\bar{\rho} \bar{W}_j) = 0$
$\Phi = \frac{C_l}{\rho}, \Gamma_{\Phi} = D_l \rho, S_{\Phi} = \dot{m}_l.$ Diffusion (concentration) equation	Initial form	$\frac{DC}{D\tau} = \frac{\partial}{\partial x_j} \left(D \frac{\partial C}{\partial x_j} \right) + \dot{m}_l$
	Reynolds form	$\frac{D\bar{C}}{D\tau} = \frac{\partial}{\partial x_j} \left(D \frac{\partial \bar{C}}{\partial x_j} - \bar{C}' \bar{W}'_j \right) + \dot{m}_l,$
$\bar{C}' \bar{W}'_j$ - turbulent diffusion transfer of concentration C_l of component l by means of the velocity fluctuation W'_j .		
<i>In the equations is used, the rule of summation according to the twice-repeating index ($i, j, k = 1, 2, 3$), and averaging is realized according to Favre; i.e. the density is used as a weight function, $D/D\tau$ - substantial derivative.</i>		

kg/m^3 ; C is the concentration, kg/m^3 ; H - specific energy, J/kg ; $V_{\mu} = 1/3\mu \cdot \text{grad}(\text{div } \vec{W})$ is volumetric coefficient of deformation; μ - dynamic viscosity, $kg/(m \cdot s)$; c_p - the heat capacity at constant pressure, $J/(kgK)$; w_r is the rate of chemical reaction per unit volume, $kg/(m^3/s)$; Q_r is the amount of heat generated per unit mass, J/kg , $q_v = w_r \cdot Q_r$ is the internal heat generation

as a result of the chemical reaction, W/m^3 ; q_R is the radiative heat flux from the radiation source, W/m^2 (during the combustion of hydrogen, $q_R = 0$, since, unlike carbon fuels, no soot is released, which is the main radiation generator); λ is the thermal conductivity, $W/(mK)$; δ_{ij} is the Kronecker delta; D_c is the diffusion coefficient, m^2/s ; \dot{m} is the power of the mass source (the rate of change in the mass of the chemical component per unit volume, $kg/(m^3s)$).

These equations, after averaging by the Favre method, take the Reynolds form (see Table 1) and form an open system to which the models are added for closure: turbulence ($k - \zeta - f$ - Hanjalić model), combustion (*CFM*- coherent flame model), nitrogen oxides NO_x formation (Zeldovich widened thermal mechanism) and the model of heat transfer in the boundary layer (Spalding-Patankar wall functions). The extended system of equations is solved using the numerical control volume method (*CVM*) [10, 11, 12].

The calculation grid was formed in accordance with the recommendations of [10]. The types of grids for combustion chamber volumes and clearance are given and analyzed in [9]. Here we only note that the optimal (in terms of modeling accuracy and calculation time) number of calculated control volumes for the gap width, for example, at $\ell = 0.2mm$, is 5-6, while their total number reaches 18 million [9]. Using a 3D workflow model implemented in AVL-FIRE 3D CRFD codes [10], thermal boundary conditions for modeling the thermal state of a piston are determined: coefficients of local heat transfer on its heat-absorbing surface and local temperatures of the working fluid at the boundary of the thermal boundary layer. After that, the 3-dimensional problem of determining the thermal state of a hydrogen engine piston is solved using the ANSYS software package. The latter is compatible with the AVL-FIRE program and requires less resolution when creating a grid and setting boundary conditions. Modeling of the thermal state of internal combustion engine parts using the ANSYS program is based on the Fourier differential equations (in the case of unsteady thermal conductivity) and Laplace (in the case of stationary thermal conductivity).

3 Flame propagation through the volume of the combustion chamber

Forced ignition by means of an electric spark at the moment $\varphi = -12^\circ$ leads to a noticeable increase in the value of the instantaneous maximum pressure of the p_z cycle, regardless of the excess air coefficient α . Obviously, with depletion of the hydrogen-air mixture, p_z decreases (Fig. 2). Numerical experiments on modeling pressure changes in the combustion chamber were carried out at different values of the gap. They showed that the maximum pressure of the working cycle, having at $\ell = 0.2mm$, in the case of a gap of $\ell = 0.35mm$, while observing the identity of the comparison conditions ($n = 3000 min^{-1}$, $\alpha = 1$), decreases from $p_z = 6.23 MPa$ to $p_z = 6.16 MPa$, i.e. by only 1 – 2%. Obviously, other indicators of the working cycle of a hydrogen engine, such as the amount of heat released during the working cycle, the rate of heat release and the maximum value of the average cylinder volume temperature of the working fluid T_z also change slightly. With increased values of the excess air coefficient ($\alpha > 1$), the effect of the gap on the characteristic parameters of the working fluid in the combustion chamber becomes even less noticeable.

The change in the excess air coefficient significantly affects the temperature field of the working fluid in the volume of the combustion chamber. Table 2 shows the instantaneous temperature fields for different time points: at the moment of ignition of the hydrogen-air mixture ($\varphi = -10^\circ$) and at the moment when the piston is at the upper dead center ($\varphi = 0^\circ$). The maximum values of local instantaneous temperatures corresponding to these moments are also indicated there. Based on the changes in temperature fields at these points in time, as well

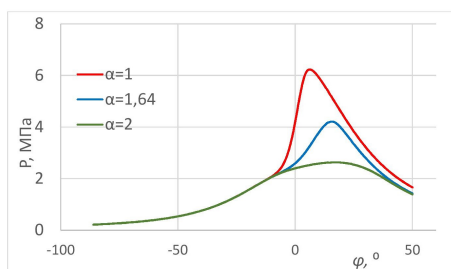
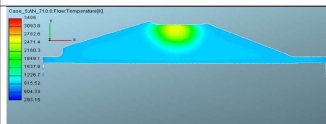
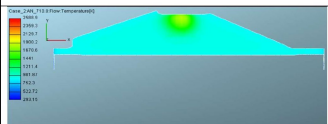
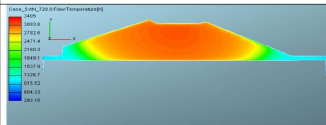
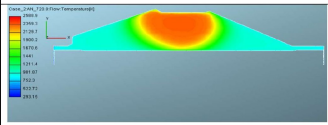


Figure 2: Cylinder pressure at $\ell = 0,2 \text{ mm}$, mode: $n = 3000 \text{ min}^{-1}$, $\alpha = \text{var.}$ $\varphi = 0^\circ$ corresponds to the upper dead center (UDC)

as taking into account the fact that the hydrogen-air mixture is homogeneous in the studied hydrogen engine with external mixing, it can be argued that:

Table 2

Instantaneous temperature fields (K) of the working fluid in the volume of the combustion chamber of a hydrogen engine as a function of the excess air coefficient α at $\ell=0,2 \text{ mm}$ and $n=3000 \text{ min}^{-1}$		
φ	$\alpha=1,0$	$\alpha=1,64$
-10°	 <p>$T_{\max}=2180 \text{ K}$</p>	 <p>$T_{\max}=1870 \text{ K}$</p>
0°	 <p>$T_{\max}=2782 \text{ K}$</p>	 <p>$T_{\max}=2359 \text{ K}$</p>

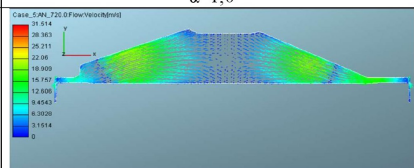
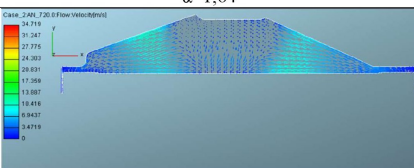
1. The rate of flame propagation through the volume of the combustion chamber, and as a result, the rate of heat release, during the combustion of a stoichiometric mixture ($\alpha = 1.0$) is significantly higher than in the case of the combustion of a depleted mixture ($\alpha = 1.64$). In this regard, in the case of $\alpha = 1.0$, the unsteady pressure in the cylinder $p(\varphi)$ reaches its maximum $p = p_z$ at $\varphi = 7^\circ$, and in the case of $\alpha = 1.64$ – at $\varphi = 15^\circ$ (see Fig. 2). The proximity of the moment of maximum pressure relative to the upper dead center indicates high efficiency of the operating cycle of the engine with a stoichiometric mixture compared with the case of a depleted mixture;

2. During the combustion of hydrogen, as well as during the combustion of traditional hydrocarbon fuels, various NO_x nitrogen oxides are formed, among which NO dominates, the proportion of which is approximately 90 – 95% of all NO_x nitrogen oxides. According to the so-called widened thermal mechanism of Ya. B. Zeldovich, NO formation occurs at temperatures $T > 1800 \text{ K}$, while the amount of NO is exponentially dependent on T . Then the nature of the change in maximum temperatures depending on the coefficient of excess air a from Table 2 allows us to assert that the high efficiency of the hydrogen working cycle (i.e., high cycle efficiency) with a stoichiometric mixture is simultaneously accompanied by low environmental friendliness, i.e., high emissions of harmful gases (nitrogen oxides NO_x). In this case, which is

called a “conflict of goals” in the theory of reciprocating engines, the use of special methods is required [13].

The instantaneous velocity fields shown in Table 3 correspond to the instantaneous temperature fields from Table 2 at the time when the piston is at top dead center, i.e. at $\varphi = 0^\circ$.

Table 3

Instantaneous velocity fields (m/s) of the working fluid in the volume of the combustion chamber of a hydrogen engine as a function of the excess air coefficient α at $\ell=0,2$ mm and $n=3000$ min ⁻¹		
φ	$\alpha=1,0$	$\alpha=1,64$
0°	 <p style="text-align: center;">$W_{\max}=22$ m/s</p>	 <p style="text-align: center;">$W_{\max}=17$ m/s</p>

The maximum values of local instantaneous velocities are also indicated there, depending on the excess air coefficient α . As can be seen, the vector fields of the working body movement in the combustion chamber are similar for stoichiometric ($\alpha = 1,0$) and depleted ($\alpha = 1,64$) mixtures (they have similar velocity vector arrangements), which is due to the invariance of the geometric shape of the combustion chamber and the location of the ignition source (electric spark plug). As for the magnitude of the local velocities, it can be seen that they are noticeably higher with a stoichiometric mixture (Table 3). Consequently, the velocity and pressure in the inlet section of the gap located between the piston and the sleeve will be greater when a flame enters it with a stoichiometric mixture.

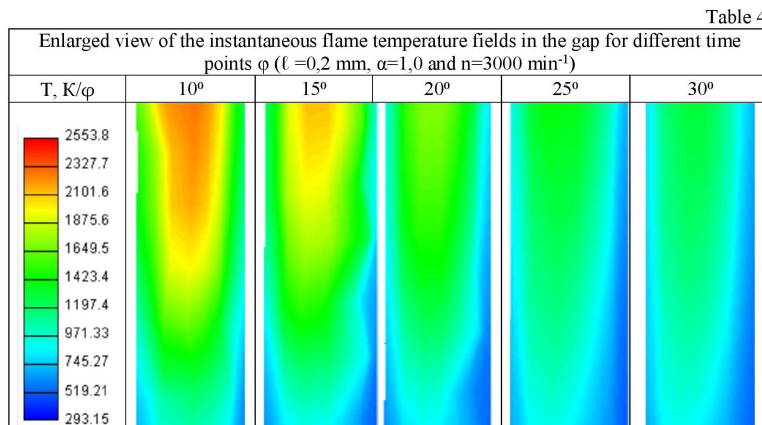
4 Flame propagation over the volume of the annular gap

The effect of flame propagation in the annular gap between the piston and the cylinder can be observed from the instantaneous temperature fields obtained for different time points φ (see Table 4). Note that at a high concentration of hydrogen ($\alpha = 1$), the flame spreads throughout the entire volume of the gap (Table 4), while the temperature drop is clearly visible in the wall layers, which is explained by the cooling effect of the gap walls. A lower temperature in the wall layers for all time points φ is observed near the surface of the cylinder liner, which is subjected to more intense liquid cooling than the surface of the piston.

It should be noted that with a depleted mixture, when $\alpha = 1.64$, only a very small amount of hydrogen burns in the inlet part of the gap, which is noticeable until time $\varphi = 10^\circ$. After this moment, despite the fact that combustion continues in the chamber volume, combustion stops at the entrance to the gap and the flame does not penetrate into the gap. With an even greater depletion of the mixture, when $\alpha = 2$, the hydrogen in the gap does not burn at all.

The combustion of hydrogen in the gap at $\alpha = 1$ is confirmed by a change in the mass fraction of hydrogen: during the rotation of the crankshaft from $\varphi = 8^\circ$ to $\varphi = 30^\circ$, almost 2/3 of the mass of hydrogen trapped in the gap burns out (see Table 5). By the time corresponding to the angle of rotation of the crankshaft $\varphi = 50^\circ$ with a stoichiometric mixture ($\alpha = 1$), there is practically no hydrogen left in the gap. This indicates that the flame has passed through the entire volume of the gap. With depleted mixtures ($\alpha = 1,64$ and $\alpha = 2$), as can be seen from Table 5, the flame does not penetrate into the gap and the gap volume is filled with an unburned hydrogen-air mixture with the maximum fraction of hydrogen for a given excess air

coefficient α .



The intensity of heat transfer between the working fluid and the gap walls, depending on the conditions of flame propagation/extinguishing into the gap, was estimated using the values of the non-stationary heat transfer coefficient $\alpha_w(\varphi)$ obtained for different values of the excess air coefficient a . Fig. 3 and 4 show the values of $\alpha_w(\varphi)$ at $a = var$ for the inner surfaces of the annular gap, which are the surfaces of the piston (Fig. 3) and the cylinder (fig. 4), shown in Fig.1.

Fig. 3 and 4 show that when the flame penetrates the gap ($\alpha = 1$), the inner surface of the annular gap is a firing surface and the values of the heat transfer coefficient $\alpha_w(\varphi)$ on this surface are high. Consequently, the heat losses to the wall at $a = 1$ are high compared to the case of a depleted mixture. At $\alpha = 1,64$ and $\alpha = 2$, as can be seen from Table 5, the flame does not penetrate into the gap and the intensity of heat transfer to the inner walls of the annular gap decreases significantly, which is confirmed by the values of the heat transfer coefficient $\alpha_w(\varphi)$ in Fig. 3 and 4.

It can be argued that the results of the study of the processes of unsteady heat transfer in the gap, shown in Fig. 3 and 4, fully explain the phenomenon of increased heat loss in hydrogen engines observed in the experiments of Professor T. Shudo, which is especially noticeable when the engine is running on a stoichiometric mixture [1, 2]. A comparison of the coefficients of unsteady heat transfer $\alpha_w(\varphi)$ shown in Fig. 3 and 4 shows that the values of $\alpha_w(\varphi)$ for the lateral firing surface of the piston F_{LFK} , which performs reciprocating motion, are in any case greater than for the surface of the firing belt of the cylinder liner F_{SFZ} (Fig.1).

Numerical experiments carried out for the ring gap with the increased size of $\ell = 0,35 \text{ mm}$ and $\ell = 0,2 \text{ mm}$ that satisfy the condition ($\ell_{crH2} \approx 0,125 \text{ mm}$) $< (\ell = 0,35 \text{ mm}) < (\ell_{crCH} \approx 0,5 \text{ mm})$, showed that the values of heat transfer coefficient in comparison with the case of $\ell = 0,2 \text{ mm}$ (Fig. 3 and 4) are reduced: on the surface of the piston to the absorption $\alpha_{wmax} = 4354 \text{ W}/(\text{m}^2 \text{ K})$ at $\varphi = 15,5^\circ$ and on the cylinder surface to the absorption $\alpha_{[wmax]} = 4368 \text{ W}/(\text{m}^2 \text{ K})$ at $\varphi = 4,5^\circ$ respectively. This result is consistent with the theory of Ya. B. Zeldovich, according to which, with an increase in the size of ℓ , heat transfer can be made arbitrarily small [5].

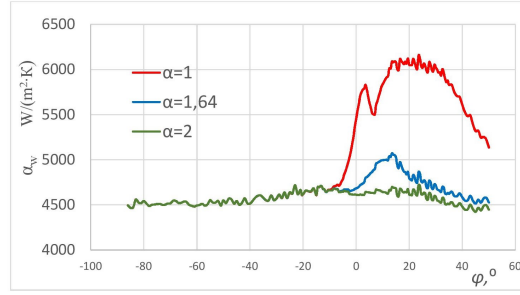
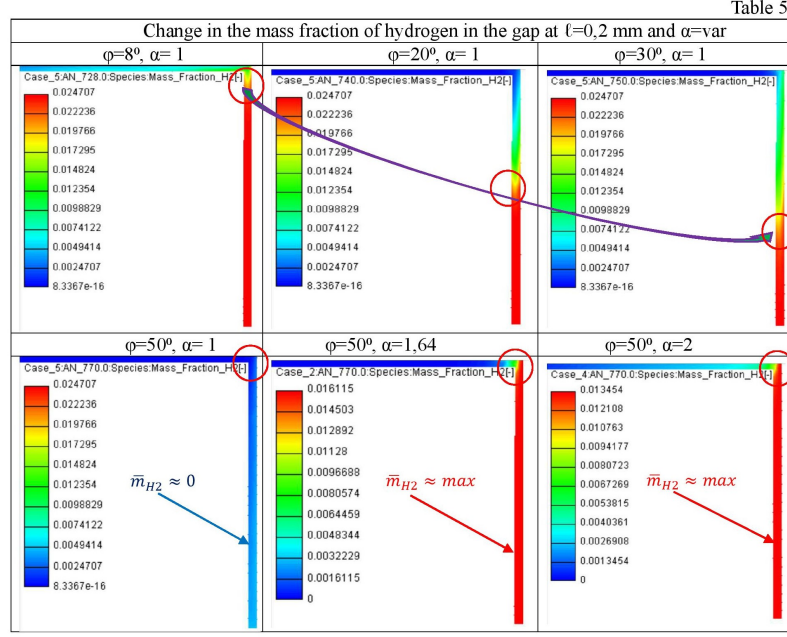


Figure 3: Heat transfer coefficient on the surface of the piston in the gap at $\ell = 0.2$ mm, mode: $n = 3000 \text{ min}^{-1}$ and $\alpha = var$ ($\alpha_{w \max} = 6125 \text{ W}/(m^2 K)$ at $\phi = 24^\circ$).

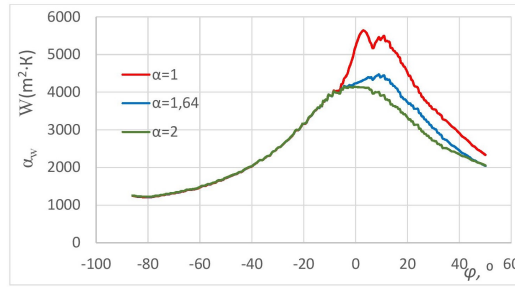


Figure 4: Heat transfer coefficient of the sleeve surface at $\ell = 0.2$ mm, mode: $n = 3000 \text{ min}^{-1}$ and $\alpha = var$ ($\alpha_{w \max} = 5546 \text{ W}/(m^2 K)$ at $\phi = 5, 5^\circ$).

5 Conclusion

The study of the problem of flame propagation/extinguishing in a narrow annular gap located above the compression ring and adjacent to the volume of the combustion chamber is relevant for determining the heat-stressed state of the piston and cylinder liner, as well as for assessing heat losses in reciprocating engines. Its solution is especially important for hydrogen engines currently being implemented at a high rate, due to the ability of the hydrogen flame to spread in narrow gaps in which the flame of the hydrocarbon fuel goes out.

Direct measurement of such characteristic flame parameters as pressure, temperature and velocity of the flame front, as well as visual observation of the process of its propagation in a narrow gap in the combustion chamber of a running engine, is a difficult, as yet unsolved task. In this paper, a solution to this problem is proposed by the method of mathematical modeling. A brief description of the 3D mathematical model used is given, based on the fundamental conservation equations of the Navier-Stokes type and previously tested on various problems of thermal power engineering, in particular the theory of heat engines.

The results obtained have both scientific and theoretical and practical significance, since they:

1. Explain the phenomenon of increased heat loss in hydrogen engines, previously observed in experimental studies by a number of authors, but who did not provide a complete theoretical explanation for this phenomenon;
2. Contain quantitative data confirming that the thermal boundary conditions on the inner surfaces of the gap for cases of penetration and extinguishing of a hydrogen flame in it differ significantly from each other. Obviously, the heat losses in the combustion chamber and the thermal loads on the main parts, primarily on the piston and cylinder liner, will also vary significantly. This should be taken into account in practice, especially when converting production engines running on traditional hydrocarbon fuels to hydrogen;
3. Indicate the possibility of controlling the processes of hydrogen flame propagation into the gap between the piston and the cylinder, reducing thermal loads on the main engine parts (piston, cylinder liner) and heat losses in the engine operating cycle by regulating the size of the gap and the composition of the hydrogen-air mixture.

Acknowledgments

This work was supported by Shota Rustaveli National Science Foundation of Georgia (Grant FR-23-8035). The author thanks Dr. Rongrong Cheng and Dr. Citian Zhang (Beijing Institute of Technology) for their help in performing the calculations.

References

- [1] T. Shudo. *Applicability of heat transfer equations to hydrogen combustion*, JSAE Review, **23**, 3 (2002), 303-308
- [2] T. Shudo. *Improving thermal efficiency by reducing cooling losses in hydrogen combustion engines*, Int. J. Hydrogen Energy, **32**, 17 (2007), 4285-4293
- [3] J. Demuyne, M. De Paepe, I. Verhaert, S. Verhelst. *Heat loss comparison between hydrogen, methane, gasoline and methanol in a spark-ignition internal combustion engine*, Energy Procedia, **29** (2012), 138-146
- [4] R.Z. Kavtaradze, D.O. Onischenko, A.S. Golosov, A.A. Zelentsov, Cheng Rongrong, and G.Zh. Sakhvadze. *The Influence of the "Piston Heat Belt-Sleeve" Gap on Heat Exchange in the Combustion Chamber of an Engine Depending on the Fuel Utilized*, Journal of Machinery Manufacture and Reliability, **51**, 2 (2022), 112-120

-
- [5] Ya.B. Zeldovich. *The theory of the limit of propagation of a silent flame: 233-246 p. /in the book: Zeldovich Ya. B. Selected works*. Chemical physics and hydrodynamics (Russian), Moskow: Publishing house Nauka, 1984, 374 p.
 - [6] I.L. Drell, F.E. Belles. *Survey of hydrogen combustion properties*, Technical Report 1383. National Advisory Committee on Aeronautics (NACA) USA, 1958, 5 p.
 - [7] C.M. White, R.R. Steeper, A.E. Lutz. *The Hydrogen-fueled internal combustion engine: a technical review*, Int. Journal of Hydrogen Energy, **31** (2006), 1292-1305
 - [8] G. Merker, Ch. Schwarz, G. Stiesch, F. Otto. *Verbrennungsmotoren: Simulation der Verbrennung und Schadstoffbildung.*, Stuttgart, Leipzig, Wiesbaden: Teubner-Verlag, 2006, 410 p.
 - [9] R. Kavtaradze, T. Natriashvili, M. Glonti, G. Chilashvili. *Flammenlöschung und Wärmeübertragung in Wasserstoff-Kolbenmotoren. Bericht auf dem Dresdner Wasserstoff-Symposium am 15.06. - 16.06.2023. Sammlung von Symposiumsberichten*. Dresden, Hochschule für Technik und Wirtschaft Dresden (HTWD), 2023, 20 p.
 - [10] FIRE. Users Manual. Version 2018. AVL List GmbH Graz, Austria, 2019
 - [11] R.Z. Kavtaradze. *Local heat transfer in piston engines (3rd edition)*. Moscow, Publishing House of Bauman Moscow State Technical University (Russian), 2016, 515 p.
 - [12] R.Z. Kavtaradze, A.M. Kondratev., Cheng Rongrong, Zhang Citian, Sun Baigang, G.Zh. Sakhvadze. *Local Heat Exchange in the Combustion Chamber of a Hydrogen Engine Running on a Lean Fuel*, Journal of Machinery Manufacture and Reliability, **50**, 1 (2021), 79-87
 - [13] R.Z. Kavtaradze, S.S. Sergeev. *New Alternative (Partially Homogeneous) Combustion Process as a Method for Reduction of Concentrations of Nitric Oxides and Soot in Combustion Products of Diesel*, High Temperature. **52**, 2 (2014), 285-299